







Rocket drops: The self-propulsion of supercooled freezing drops

Claudiu A. Stan ^{1,2,*}, Armin Kalita ¹, Sebastian Marte ¹, Thomas F. Kaldawi ¹,
Philip R. Willmott ^{3,4} and Sébastien Boutet ³

¹*Department of Physics, Rutgers University–Newark, Newark, New Jersey 07102, USA*

²*Stanford PULSE Institute, SLAC National Accelerator Laboratory, Menlo Park, California 94025, USA*

³*Linac Coherent Light Source, SLAC National Accelerator Laboratory, Menlo Park, California 94025, USA*

⁴*Paul Scherrer Institute, CH-5232 Villigen, Switzerland*



(Received 1 November 2022; accepted 4 January 2023; published 3 February 2023)

Isolated supercooled water drops have been observed to move spontaneously while freezing in vacuum. This motion is caused by an increase of the evaporation rate during the early stages of freezing, which transfers momentum to the drops, similar to rocket propulsion. As in other cases of self-propulsion, symmetry breaking is necessary, and occurs when ice nucleation occurs away from the center of the drop. The self-propulsion velocity was modeled analytically for a simplified case, and numerically for two experiments. The model predicts peak velocities on the order of 1 m/s in vacuum, and a drop kinematics similar to that observed experimentally. In air, the self-propulsion velocity is expected to be much smaller but may be detectable for micron-sized drops.

DOI: [10.1103/PhysRevFluids.8.L021601](https://doi.org/10.1103/PhysRevFluids.8.L021601)

Liquid droplets can exhibit spontaneous motions near solid and liquid surfaces [1–5], or when immersed in another liquid [6,7]. When the droplet and its environment appear symmetric, these motions are counterintuitive [3,8] because the force driving the motion should average out. But on closer inspection, such cases of self-propulsion were found to be caused by the breaking of the system's symmetry, which can be due to the spontaneous formation of thermal or chemical gradients [7,8], or due to localized evaporation from the drop [3–5]. In particular, localized evaporation provides a relatively strong force [9,10] and a local pressure buildup that can lead to the Leidenfrost effect and to some of the most rapid cases of self-propulsion [1,2,11]. While the Leidenfrost effect is usually observed in proximity to hot surfaces, evaporation can also provide strong forces at cryogenic temperatures [5] or in a low-pressure environment [4].

Here, we investigate a spontaneous motion of isolated drops in vacuum. This motion, which occurs when supercooled drops freeze after ice nucleation, is caused by a localized increase in the evaporation rate as the freezing drop temporarily heats (recalesces) to the melting temperature [12]. The spherical symmetry of this process is broken if nucleation occurs away from the center of the drop, which leads to a net reactive force, the same as in rocket propulsion [13]. The fastest self-propulsion due to freezing will occur when nucleation occurs at the surface, but the average self-propulsion is also significant. On average, substantial symmetry breaking occurs even when nucleation is equally probable inside the drop, because the volume-averaged radial position of the nucleation is at three-quarters of the drop radius.

We investigated the reactive propulsion of freezing drops by imaging optically [14,15] a stream of 40.9- μm -diameter water drops injected downward with an initial speed of 9.9 m/s into a vacuum chamber at 0.4 Pa. The velocity change due to gravitational acceleration was negligible relative

*claudiu.stan@rutgers.edu

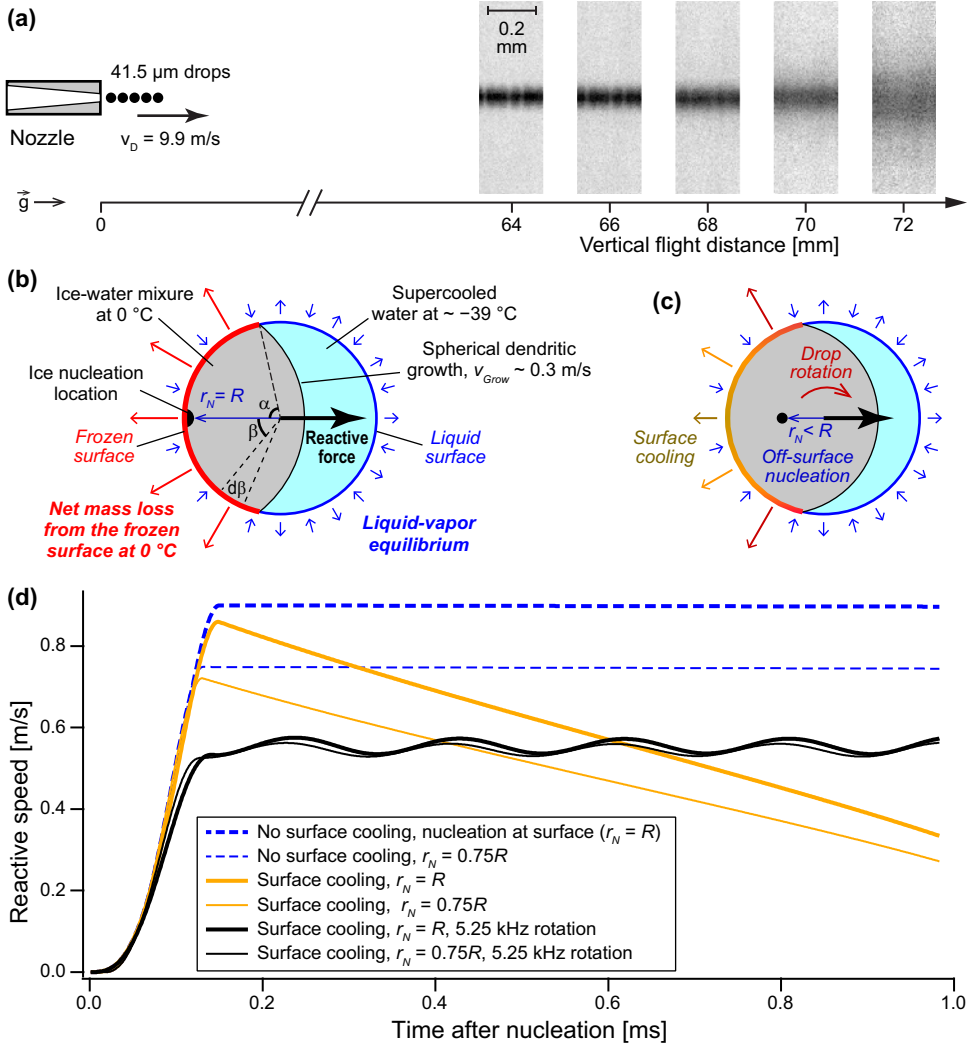


FIG. 1. Observation and modeling of the reactive self-propulsion of freezing drops. (a) Spreading of a train of drops after they froze. The images are averages of multiple drop stream images synchronized with the generation of drops, and cover the range of flight distances over which the drops nucleate ice and start to freeze. (b) A simplified physical model of the reactive force due to enhanced evaporation during freezing. (c) Additional mechanisms that impact the reactive force. (d) The evolution of the self-propulsion speed from ice nucleation until complete solidification, for a 40.9- μm -diameter drop supercooled to 234 K.

to the injection and self-propulsion velocities, because the self-propulsion was investigated over a short time interval (~ 1 ms). To determine the velocity of individual drops, each image was exposed to 2 or 12 light pulses (462 nm wavelength, 100 ns duration) at 5 μs intervals. Up to 12 vertically displaced images of the same drop thus appeared in one image [14]. Images were recorded at both low and high magnifications (5.1 and 0.497 $\mu\text{m}/\text{pixel}$, respectively). The experiments were conducted at the Coherent X-ray Imaging instrument of the Linac Coherent Light Source [16,17].

We initially observed the self-propulsion of freezing drops as a sudden lateral spreading of the drop stream after freezing. Figure 1(a) shows averages of ~ 1000 low-magnification images of the

drop stream at different distances from the nozzle. Since the images were synchronized with the production of the drops, the pattern along the stream in the averaged images indicates that the drop velocities along the stream remained constant during flight. The pattern coexisted with a slight lateral spreading, which we hypothesize was caused by the electrostatic repulsion of the drops after they acquired a streaming potential at the nozzle. After 68 mm of travel, the longitudinal patterning started to disappear while the lateral spread of the stream increased rapidly, which indicates that the drops acquired an additional, and randomly oriented, self-propulsion velocity. We confirmed using images recorded at high magnification [14] that the drops froze within the range of flight distances displayed in Fig. 1(a).

The spontaneous motion of free water drops freezing in vacuum was also observed in other studies. Ando *et al.* recorded the flight trajectory of a drop while it froze and showed that it changed direction after ice nucleation [18]. In an experiment that used water drops in vacuum to collect x-ray scattering data from supercooled water, the rate at which a narrow x-ray beam intersected the drops decreased rapidly after the drops froze [19], indicating a spreading of the drop stream. Spontaneous motion due to the freezing of supercooled drops at low pressures can also occur near surfaces. A high-speed movie from Wildeman *et al.* [20] shows a drop moving away from the silver iodide tip that was used to trigger nucleation on its surface. Schutzius *et al.* [4] reported the self-detachment of freezing drops from a range of surfaces at low pressures, and explained that the increase in evaporation, due to recalescence, built up an overpressure between the drop and the surface, which provided the self-detachment force.

The freezing of supercooled drops is a multistage process, which starts with a stage of dendritic freezing during which part of the liquid freezes and the drop heats to the melting temperature (recalesces), followed by the complete solidification of the drops [12,20–22]. During the latter stage, the drops may eject material or shatter [20,23,24], which would impart a velocity to the drop due to the conservation of momentum, and would cause the drop stream to spread. Nevertheless, the reactive self-propulsion of the drop during the dendritic stage of freezing is a distinct phenomenon. This is most clearly shown in the drop trajectory reported by Ando *et al.* [18], where the trajectory changed before the drop shattered.

A simplified case of reactive self-propulsion that can be modeled analytically is illustrated in Fig. 1(b). A supercooled water drop surrounded by water vapor at the saturated vapor pressure of the supercooled liquid starts to freeze after ice nucleates at the surface. We assume that the drop is sufficiently supercooled that the ice grows as a network of fine dendrites, which occurs in water supercooled below -10°C [25]. We also assume that the region with dendritic ice grows spherically, which is consistent with the growth observed in $\sim 100\text{-}\mu\text{m}$ -diameter drops freezing at -35°C [26]. This assumption may apply only to small drops at large supercooling, as deviations from spherical growth were observed in larger drops near -20°C [4,24]. During growth, the drop is divided into a supercooled liquid region at its initial temperature and a mixture of liquid and dendrites at the melting temperature of 0°C . Such regions, at the initial supercooling and recalesced to 0°C , were observed experimentally in water drops using thermal imaging [4,24], and the transition between regions was modeled to be on the order of $1\ \mu\text{m}$ thick [27]. We further assume that the drop surface is solid ice where it bounds the region with dendrites and liquid otherwise, and that the frozen surface remains at the melting temperature while the temperature of the liquid surface stays constant. Since ice at the melting temperature has a larger vapor pressure than supercooled water [28], the evaporative flux from the drop will be asymmetric and the drop will experience a net reactive force directed opposite to the nucleation point.

The instantaneous reactive force at an elapsed time t after nucleation is given by the integral of the reactive force contributions over the frozen surface. For simplicity, we assume that the pressure is low enough that the evaporative flux is in the free molecular regime, a condition under which the net evaporation rate is proportional to the difference between the saturated vapor pressure and the ambient vapor pressure [19]. In this case, the normal reactive force per unit area of frozen surface is equal to half of the pressure difference between the saturated vapor pressure of ice at the melting point, p_{ice} , and the saturated vapor pressure of the supercooled water, p_{scw} . The polar

angle of the most advanced frozen points on the surface is $\alpha(t) = \pi - 2 \arccos [(v_{\text{grow}} t)/(2R)]$, where nucleation occurs at $\alpha = 0$, v_{grow} is the dendrite growth speed [25], and R is the drop radius. The reactive force contribution dF from a polar sector of the sphere at an angle β and width $d\beta$ is given by $dF = \pi R^2 (p_{\text{ice}} - p_{\text{scw}}) \cos(\beta) \sin(\beta) d\beta$. Integration over all frozen sectors leads to the instantaneous reactive force $F(t)$,

$$F(t) = (1/2)\pi R^2 (p_{\text{ice}} - p_{\text{scw}}) \sin^2 \alpha(t). \quad (1)$$

The linear momentum acquired by the drop is obtained by integrating $F(t)$ until the drop is filled with ice dendrites at $t_{\text{final}} = 2R/v_{\text{grow}}$. Defining an integration variable $x = v_{\text{grow}} t/(2R)$, the final velocity in this simplified scenario, Δv_{max} , is given by

$$\Delta v_{\text{max}} = \frac{3}{4} \frac{(p_{\text{ice}} - p_{\text{scw}})}{\rho v_{\text{grow}}} \int_0^1 \sin^2(\pi - 2 \arccos x) dx = \frac{2}{5} \frac{(p_{\text{ice}} - p_{\text{scw}})}{\rho v_{\text{grow}}}, \quad (2)$$

where ρ is the density of supercooled water. If the evaporation remains in the free molecular regime, Eq. (2) remains valid at ambient vapor pressures that are different from the saturated pressure of the supercooled liquid, because the momentum conservation force due to vapor condensation averages to zero for the entire drop.

The simplified model predicts that the reactive force accelerates the drop during the dendritic growth phase, after which the reactive self-propulsion velocity remains constant. The final velocity is equal to Δv_{max} , which according to Eq. (2) is 0.85 m/s at -40°C . In experiments, Δv_{max} is an upper limit, and Fig. 1(c) illustrates a few mechanisms that reduce the reactive velocity: (i) nucleation can occur anywhere inside the drop, which reduces the duration of the reactive force; (ii) the frozen surface cools, which reduces the magnitude of the reactive force; and (iii) the reactive velocity can be further reduced if the drop rotates. We modeled numerically the impact of these mechanisms for conditions typical to our experiment, and Fig. 1(d) shows how the self-propulsion speed varies under different scenarios, from ice nucleation until the drop is fully solidified.

An equally probable nucleation within the drop volume has a relatively small impact on the self-propulsion velocity because most of the volume of a sphere is relatively close to its surface. Since the volume-averaged radial distance in a sphere is equal to 0.75 of its radius, we evaluated the effect of random nucleation by integrating numerically the time-dependent reactive force for nucleation occurring at $0.75R$ from the drop center. The self-propulsion velocity was reduced by less than one-quarter compared to the case of surface nucleation.

The impact of the surface cooling is both quantitative and qualitative. We modeled its effect by approximating that the surface temperature evolved the same as during symmetric postdendritic solidification. We calculated the surface temperatures during solidification [14,24], and used them to determine the position- and time-dependent vapor pressure along the surface, the time-dependent reactive force, and the reactive velocity. Figure 1(d) displays the reactive velocity for nucleation at the surface and at $0.75R$ from the drop center. The reactive velocity reaches a peak approximately when the dendritic ice growth ends, then it decreases. The peak occurs because surface areas that froze later are warmer and have relatively larger evaporation rates. After the surface freezes completely, the temperature differences generate a reactive force that is opposite to the initial force and decelerates the drop.

The freezing drop trajectory reported by Ando *et al.* [18] displays a sharp bend shortly after ice nucleation, followed by a more gradual bending with an opposite curvature. This trajectory is consistent with our model when the effect of surface cooling is included. Figure 2(a) compares points sampled along the experimental trajectory with a trajectory calculated using the reactive force model with surface cooling. The direction of the reactive velocity and the radial location of nucleation cannot be measured from the trajectory, and were determined by fitting the experimental trajectory against our model [14]. The quantitative agreement with the model is very good, but this could be partly due to using multiple free parameters to model the trajectory.

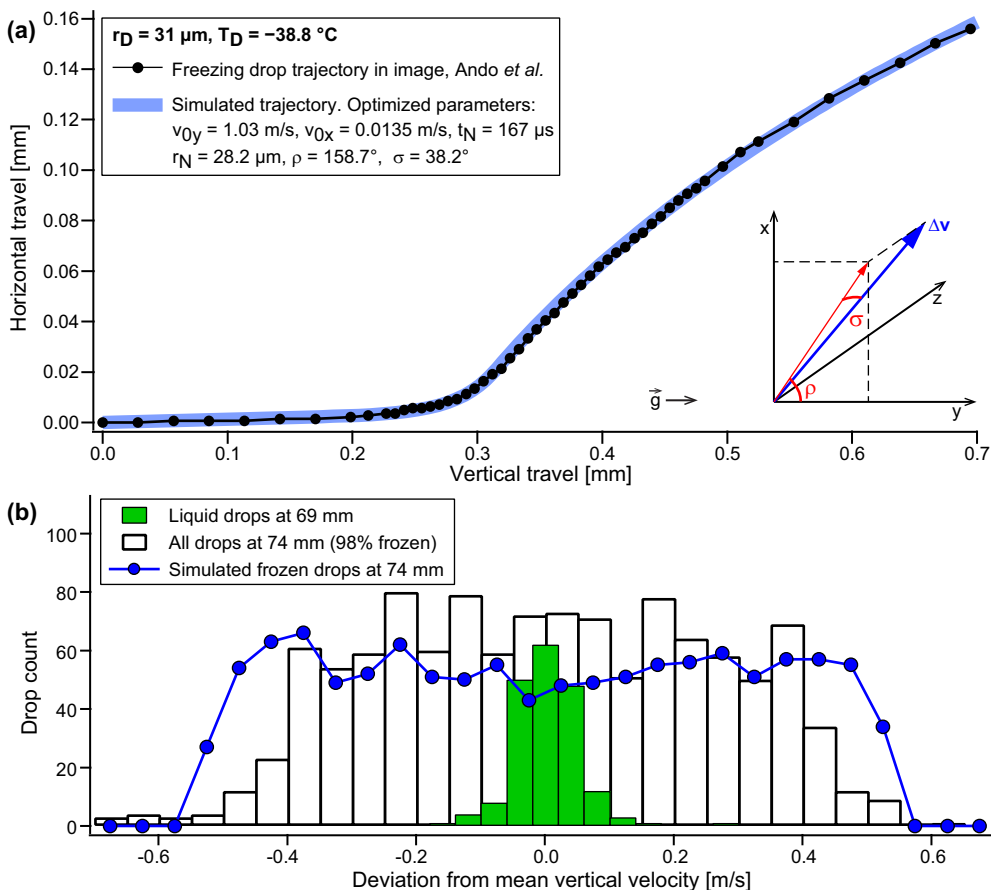


FIG. 2. Comparison of the reactive self-propulsion model with experimental data. (a) Comparison between the trajectory of a 62- μ m freezing drop observed by Ando *et al.* [18], and the trajectory predicted by the model. (b) The experimental distributions of vertical velocities of liquid drops at 69 mm and of frozen drops at 74 mm, and the distribution predicted by the self-propulsion model at 74 mm.

The drops in our experiment, which were produced by driving the Rayleigh breakup of a liquid jet, rotated at a frequency of 5.25 kHz [14]. The rotation can be explained by a reproducible asymmetry of the Rayleigh breakup. We modeled the effect of rotation by integrating numerically the Cartesian components of the reactive velocity during freezing [14]. Figure 1(d) shows the magnitude of the velocity when the reactive force is perpendicular to the rotation axis. If the reactive force is parallel to the rotation axis, the rotation does not affect the direction of the force and the velocity is the same as without rotation. For an arbitrary orientation of the rotation axis, the magnitude of the reactive velocity has values intermediate between the perpendicular and the parallel cases.

We tested the reactive velocity model against our data by determining the vertical velocity distribution of drops before and after freezing [14,29]. To obtain accurate velocity measurements we used high magnification images, rather than the low-magnification data sets used in Fig. 1(a). We had high magnification images only at 69 mm (2 exposures) and 74 mm (12 exposures) of travel, and only the 2-exposure data at 69 mm had sufficiently low noise to identify liquid drops [14]. After 69 mm of travel, 53% of the drops were observed to be frozen, consistent with the freezing probability expected for homogeneous ice nucleation [26,30,31]. Given that the spread

of homogeneous nucleation times is approximately 1 ms in our experiment, and that the 74 mm data is recorded 0.5 ms later during flight than the 69 mm data (where more than half of the drops were frozen), almost all the drops in the 74 mm data set were frozen. Statistically, we estimated that 98% of the drops at 74 mm nucleated ice [14], thus the 74 mm data represents to a good approximation the behavior of frozen drops. The velocity distributions for liquid and frozen drops are shown in Fig. 2(b) along with a velocity distribution modeled with surface cooling, rotation, and random directions of the reactive force. The velocity distribution broadens after freezing due to the randomly oriented self-propulsion, and it is consistent with but narrower than a distribution simulated based on our self-propulsion model. The wider distribution in the model indicates that it may overestimate the self-propulsion velocity, but we consider the agreement to be satisfactory given the simplifications made in the model. The overestimation of the velocity could be due to the dendrite growth speed being inaccurate or due to a nonspherical growth of the mixed phase [14]. We note that the velocities modeled in Fig. 2(b) consider the location of the image plane, which did not overlap with the center of the drop stream [14]. Due to this misalignment, drops were visible only if they traveled perpendicular to the image plane after nucleation. The imaged drops thus had a velocity component along the imaging axis, and this reduced the velocities observed in the image plane.

With peak velocities on the order of 1 m/s, the reactive motion of freezing drops in vacuum is faster than the self-propulsion caused by chemical or thermal gradients [6,8], and is comparable to the fastest self-propulsion phenomena [1,2,5,11] driven by evaporation near surfaces. The self-propulsion is powered by the release of latent heat during freezing. It has a very small thermal efficiency, approximately five orders of magnitude smaller than the efficiency of a corresponding Carnot cycle [14]. The low efficiency can be explained by the wide angular spread of the reactive force components and by the briefness of the dendritic growth, which is the most asymmetric stage of freezing. For a higher efficiency, the supercooled liquid could be placed in an impermeable container with a small opening, which would maintain the direction of the reactive force throughout the entire solidification process.

We expect that the reactive velocity will be greatly reduced at atmospheric pressure, because the evaporative reaction forces increase with the rate of evaporation [9,10]. The sublimation rate of ice in air is diffusion limited [32] and much smaller than in vacuum, but may be significant for small drops, where the diffusion-limited sublimation rate becomes inversely proportional to the drop radius [33]. We estimated that drops with radii on the order of 10 μm , a size typical to drops in clouds [12], will acquire velocities on the order of 1% of the velocities in vacuum [14]. We do not expect that the reactive self-propulsion has a significant role in cloud drop dynamics because other self-propulsion processes such as drop shattering produce faster ice particles [20,21].

The self-propulsion of freezing drops is detrimental to experiments that use drops in vacuum to study deeply supercooled water and its freezing [19,34,35], because it can lead to a reduction in the data rate or in the signal intensity. The self-propulsion model could help optimize such experiments, for example, by predicting where a drop stream should be probed to collect data most efficiently. The model can also inform experiments on the self-detachment of freezing drops from solid surfaces [4], because it allows the treatment of cases where ice nucleation is not facing the solid surface and the overpressure between the drop and the surface would not develop.

The experiments were supported by the U.S. Department of Energy, Office of Science, Chemical Sciences, Geosciences, and Biosciences Division. Data analysis and interpretation were primarily supported by startup funds from Rutgers University–Newark. Supplement funding for this project was provided by the Rutgers University–Newark Chancellor’s Research Office. Use of the Linac Coherent Light Source (LCLS), SLAC National Accelerator Laboratory, is supported by the U.S. Department of Energy, Office of Science, Office of Basic Energy Sciences under Contract No. DE-AC02-76SF00515.

-
- [1] H. Linke, B. J. Aleman, L. D. Melling, M. J. Taormina, M. J. Francis, C. C. Dow-Hygelund, V. Narayanan, R. P. Taylor, and A. Stout, Self-Propelled Leidenfrost Droplets, *Phys. Rev. Lett.* **96**, 154502 (2006).
- [2] G. Lagubeau, M. Le Merrer, C. Clanet, and D. Quere, Leidenfrost on a ratchet, *Nat. Phys.* **7**, 395 (2011).
- [3] A. Bouillant, T. Mouterde, P. Bourriane, A. Lagarde, C. Clanet, and D. Quere, Leidenfrost wheels, *Nat. Phys.* **14**, 1188 (2018).
- [4] T. M. Schutzius, S. Jung, T. Maitra, G. Graeber, M. Kohme, and D. Poulikakos, Spontaneous droplet trampolining on rigid superhydrophobic surfaces, *Nature (London)* **527**, 82 (2015).
- [5] A. Gauthier, C. Diddens, R. Proville, D. Lohse, and D. van der Meer, Self-propulsion of inverse Leidenfrost drops on a cryogenic bath, *Proc. Natl. Acad. Sci. USA* **116**, 1174 (2019).
- [6] T. Toyota, N. Maru, M. M. Hanczyc, T. Ikegami, and T. Sugawara, Self-propelled oil droplets consuming “fuel” surfactant, *J. Am. Chem. Soc.* **131**, 5012 (2009).
- [7] B. Reichert, J.-B. Le Cam, A. Saint-Jalmes, and G. Pucci, Self-Propulsion of a Volatile Drop on the Surface of an Immiscible Liquid Bath, *Phys. Rev. Lett.* **127**, 144501 (2021).
- [8] Z. Izri, M. N. van der Linden, S. Michelin, and O. Dauchot, Self-Propulsion of Pure Water Droplets by Spontaneous Marangoni-Stress-Driven Motion, *Phys. Rev. Lett.* **113**, 248302 (2014).
- [9] H. J. Palmer, The hydrodynamic stability of rapidly evaporating liquids at reduced pressure, *J. Fluid Mech.* **75**, 487 (1976).
- [10] S. G. Kandlikar, Evaporation momentum force and its relevance to boiling heat transfer, *J. Heat Transfer* **142**, 100801 (2020).
- [11] V. J. Leon and K. K. Varanasi, Self-Propulsion of Boiling Droplets on Thin Heated Oil Films, *Phys. Rev. Lett.* **127**, 074502 (2021).
- [12] H. R. Pruppacher and J. D. Klett, *Microphysics of Clouds and Precipitation* (Springer, Dordrecht, 2010).
- [13] R. H. Goddard, A method of reaching extreme altitudes, *Nature (London)* **105**, 809 (1920).
- [14] See Supplemental Material at <http://link.aps.org/supplemental/10.1103/PhysRevFluids.8.L021601> for details of the experimental setup, data processing, and modeling of the self-propulsion velocity.
- [15] C. A. Stan, D. Milathianaki, H. Laksmono, R. G. Sierra, T. A. McQueen, M. Messerschmidt, G. J. Williams, J. E. Koglin, T. J. Lane, M. J. Hayes *et al.*, Liquid explosions induced by x-ray laser pulses, *Nat. Phys.* **12**, 966 (2016).
- [16] P. Emma, R. Akre, J. Arthur, R. Bionta, C. Bostedt, J. Bozek, A. Brachmann, P. Bucksbaum, R. Coffee, F. J. Decker *et al.*, First lasing and operation of an ångstrom-wavelength free-electron laser, *Nat. Photonics* **4**, 641 (2010).
- [17] M. N. Liang, G. J. Williams, M. Messerschmidt, M. M. Seibert, P. A. Montanez, M. Hayes, D. Milathianaki, A. Aquila, M. S. Hunter, J. E. Koglin *et al.*, The Coherent X-ray Imaging instrument at the Linac Coherent Light Source, *J. Synchrotron Radiat.* **22**, 514 (2015).
- [18] K. Ando, M. Arakawa, and A. Terasaki, Freezing of micrometer-sized liquid droplets of pure water evaporatively cooled in a vacuum, *Phys. Chem. Chem. Phys.* **20**, 28435 (2018).
- [19] J. A. Sellberg, C. Huang, T. A. McQueen, N. D. Loh, H. Laksmono, D. Schlessinger, R. G. Sierra, D. Nordlund, C. Y. Hampton, D. Starodub *et al.*, Ultrafast x-ray probing of water structure below the homogeneous ice nucleation temperature, *Nature (London)* **510**, 381 (2014).
- [20] S. Wildeman, S. Sterl, C. Sun, and D. Lohse, Fast Dynamics of Water Droplets Freezing from the Outside In, *Phys. Rev. Lett.* **118**, 084101 (2017).
- [21] A. Korolev and T. Leisner, Review of experimental studies of secondary ice production, *Atmos. Chem. Phys.* **20**, 11767 (2020).
- [22] T. Buttersack, V. C. Weiss, and S. Bauerecker, Hypercooling temperature of water is about 100 K higher than calculated before, *J. Phys. Chem. Lett.* **9**, 471 (2018).
- [23] A. Lauber, A. Kiselev, T. Pander, P. Handmann, and T. Leisner, Secondary ice formation during freezing of levitated droplets, *J. Atmos. Sci.* **75**, 2815 (2018).
- [24] J. Kleinheins, A. Kiselev, A. Keinert, M. Kind, and T. Leisner, Thermal imaging of freezing drizzle droplets: Pressure release events as a source of secondary ice particles, *J. Atmos. Sci.* **78**, 1703 (2021).
- [25] H. R. Pruppacher, Interpretation of experimentally determined growth rates of ice crystals in supercooled water, *J. Chem. Phys.* **47**, 1807 (1967).

- [26] C. A. Stan, G. F. Schneider, S. S. Shevkoplyas, M. Hashimoto, M. Ibanescu, B. J. Wiley, and G. M. Whitesides, A microfluidic apparatus for the study of ice nucleation in supercooled water drops, *Lab Chip* **9**, 2293 (2009).
- [27] T. Buttersack and S. Bauerecker, Critical radius of supercooled water droplets: On the transition toward dendritic freezing, *J. Phys. Chem. B* **120**, 504 (2016).
- [28] D. M. Murphy and T. Koop, Review of the vapour pressures of ice and supercooled water for atmospheric applications, *Q. J. R. Meteorol. Soc.* **131**, 1539 (2005).
- [29] C. A. Stan, P. R. Willmott, H. A. Stone, J. E. Koglin, M. Liang, A. L. Aquila, J. S. Robinson, K. L. Gumerlock, G. Blaj, R. G. Sierra *et al.*, Negative pressures and spallation in water drops subjected to nanosecond shock waves, *J. Phys. Chem. Lett.* **7**, 2055 (2016).
- [30] D. E. Hagen, R. J. Anderson, and J. L. Kassner, Homogeneous condensation–Freezing nucleation rate measurements for small water droplets in an expansion cloud chamber, *J. Atmos. Sci.* **38**, 1236 (1981).
- [31] P. Stockel, I. M. Weidinger, H. Baumgartel, and T. Leisner, Rates of homogeneous ice nucleation in levitated H₂O and D₂O droplets, *J. Phys. Chem. A* **109**, 2540 (2005).
- [32] J. Nelson, Sublimation of ice crystals, *J. Atmos. Sci.* **55**, 910 (1998).
- [33] I. Langmuir, The Evaporation of Small Spheres, *Phys. Rev.* **12**, 368 (1918).
- [34] H. Laksmono, T. A. McQueen, J. A. Sellberg, N. D. Loh, C. Huang, D. Schlesinger, R. G. Sierra, C. Y. Hampton, D. Nordlund, M. Beye *et al.*, Anomalous behavior of the homogeneous ice nucleation rate in “no-man’s land,” *J. Phys. Chem. Lett.* **6**, 2826 (2015).
- [35] N. Esmacildoost, O. Joansson, T. A. McQueen, M. Ladd-Parada, H. Laksmono, N. T. Loh, and J. A. Sellberg, Heterogeneous ice growth in micron-sized water droplets due to spontaneous freezing, *Crystals* **12**, 65 (2022).